Extended data Fig 1.

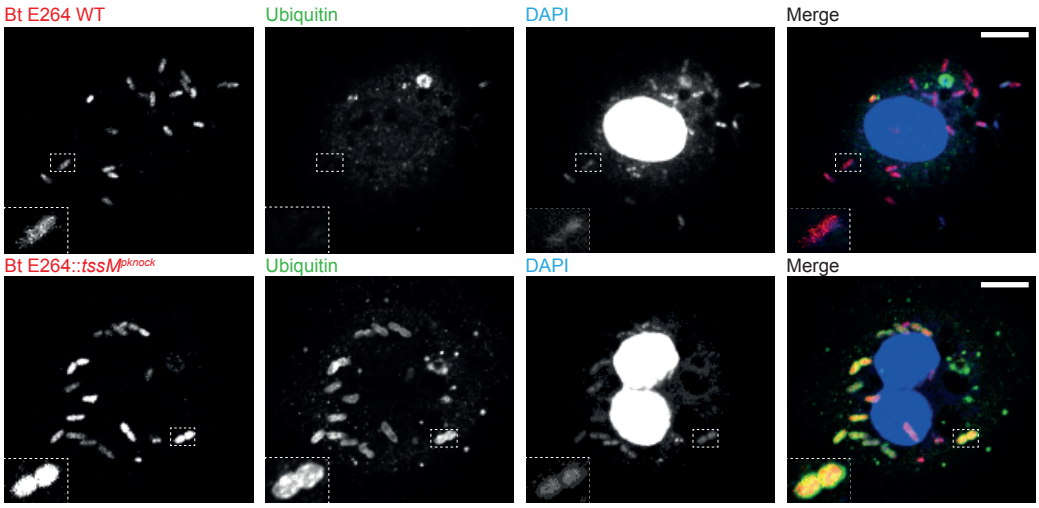

Szczesna et al., extended data Figures and legends

Extended Data Fig. 1: Ubiquitylation of Bt E264::*tssM*^{pknock} mutant bacteria. Representative confocal microscopy images of MEFs infected with *B. thailandensis* E264 (top panel) and E264::*tssM*^{pknock} (bottom panel) strains carrying the pH4-GroS-RFP plasmid. Cells were fixed at 6 h p.i. and labelled with an anti-ubiquitin antibody (green) and DAPI (blue). Scale bar - 10 μm.

Extended data Fig 2.

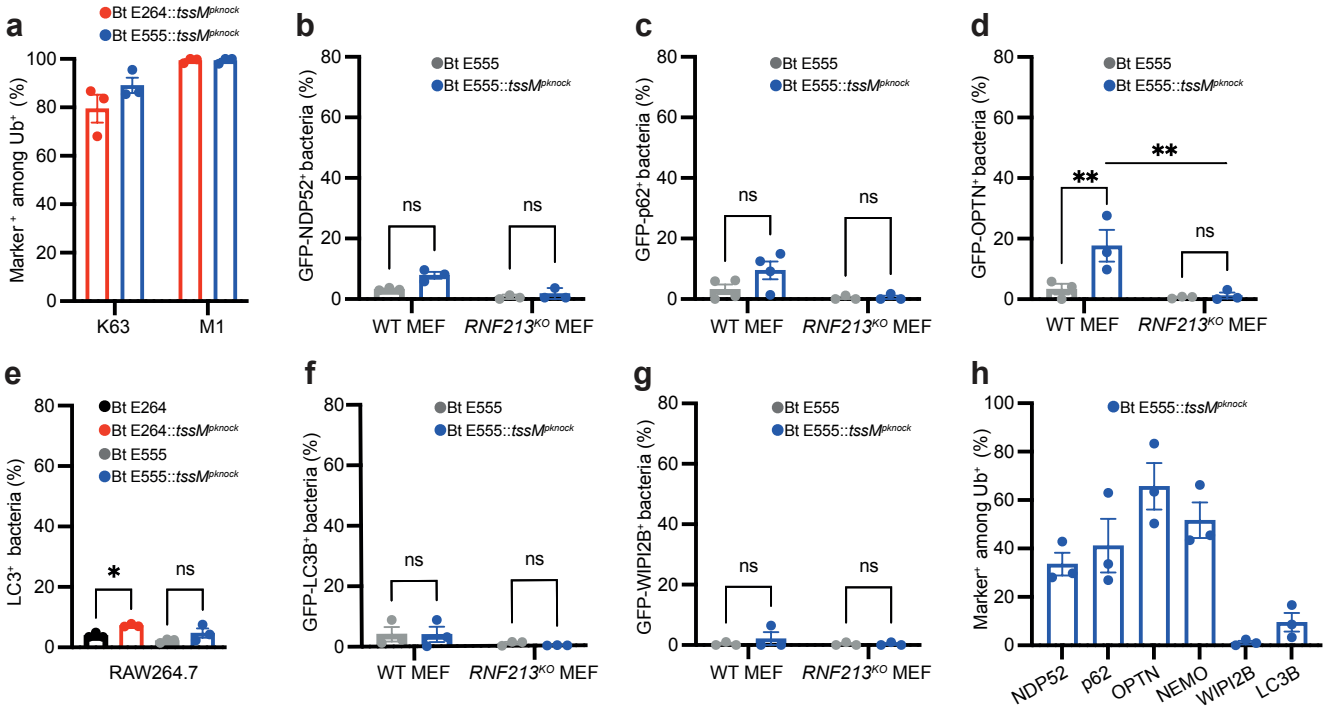

Extended Data Fig. 2: E555::*tssM*^{pknock} mutants remain poor targets for antibacterial autophagy. a) Quantification of the percentage of K63-linked and M1-linked ubiquitin-positive bacteria among those bacteria immunolabelled with a non-specific anti-ubiquitin antibody. **b-d**) Quantification of the percentage of Bt E555 WT or E555::*tssM*^{pknock} bacteria colocalising with **b)** GFP-NDP52, **c)** GFP-p62 and **d)** GFP-OPTN in WT and RNF213^{KO} MEFs at 6 h p.i. **e)** Percentage of LC3-positive bacteria in RAW264.7 macrophages at 6 h p.i. **f-g)** Quantification of the percentage of Bt E555 WT or E555::*tssM*^{pknock} bacteria colocalising **f)** GFP-LC3B and **g)** GFP-WIPI2B in WT and RNF213^{KO} MEFs at 6 h p.i. **h)** Percentage of marker-positive E555::*tssM*^{pknock} bacteria among ubiquitin-coated bacteria in WT MEFs. Data represent the mean and SEM of at least three independent biological repeats. Statistical significance was assessed by two-way ANOVA with Tukey's multiple comparisons test; * $P < 0.05$; *** < 0.001.

Extended data Fig 3.

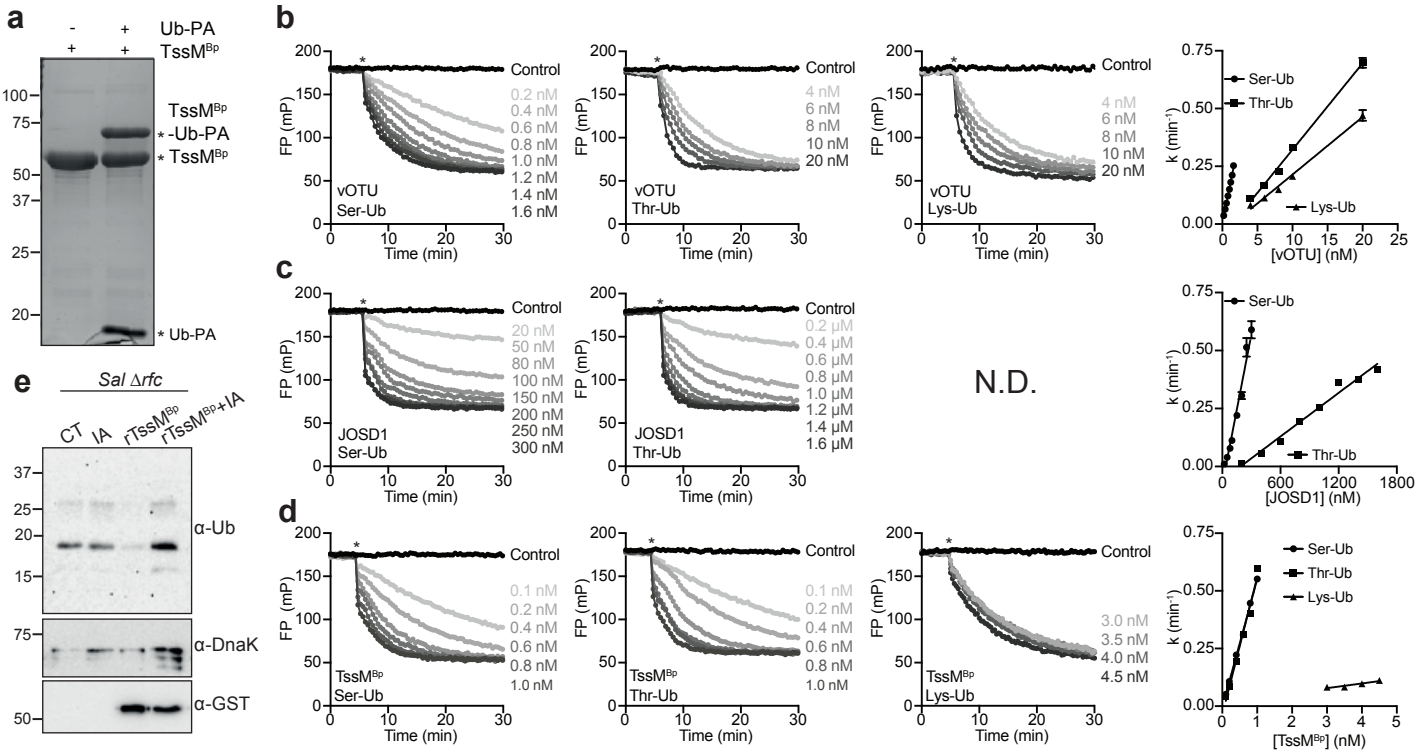

Extended Data Fig. 3: vOTU, JOSD1, and TssM^{Bp} cleave substrates with different efficiencies. a) Coomassie-stained gel of purified recombinant TssM$^{Bp\Delta N191}$ (TssM^{Bp}) incubated with and without the activity-based probe, Ub-Propargylamide (Ub-PA). **b-d)** FP curves for reactions containing 50 nM substrate with the indicated concentrations of DUB. In each panel, the darkest and lightest curves represent the highest and lowest concentrations, respectively, tested for **b)** vOTU, **c)** JOSD1, and **d)** TssM$^{Bp\Delta N191}$ (TssM^{Bp}). Rate constant derivations are shown on the far right of each panel for Ser- (circle), Thr- (square), and Lys (triangle)-linked Ub substrates. The addition of the DUB is marked with an asterisk (*). **e)** Immunoblot analysis of Δ*rfc Salmonella* isolated from infected cells and treated with recombinant His-GST-tagged TssM$^{Bp\Delta N191}$ (rTssM^{Bp}) +/- iodoacetamide for 30 min.

Extended data Fig 4.

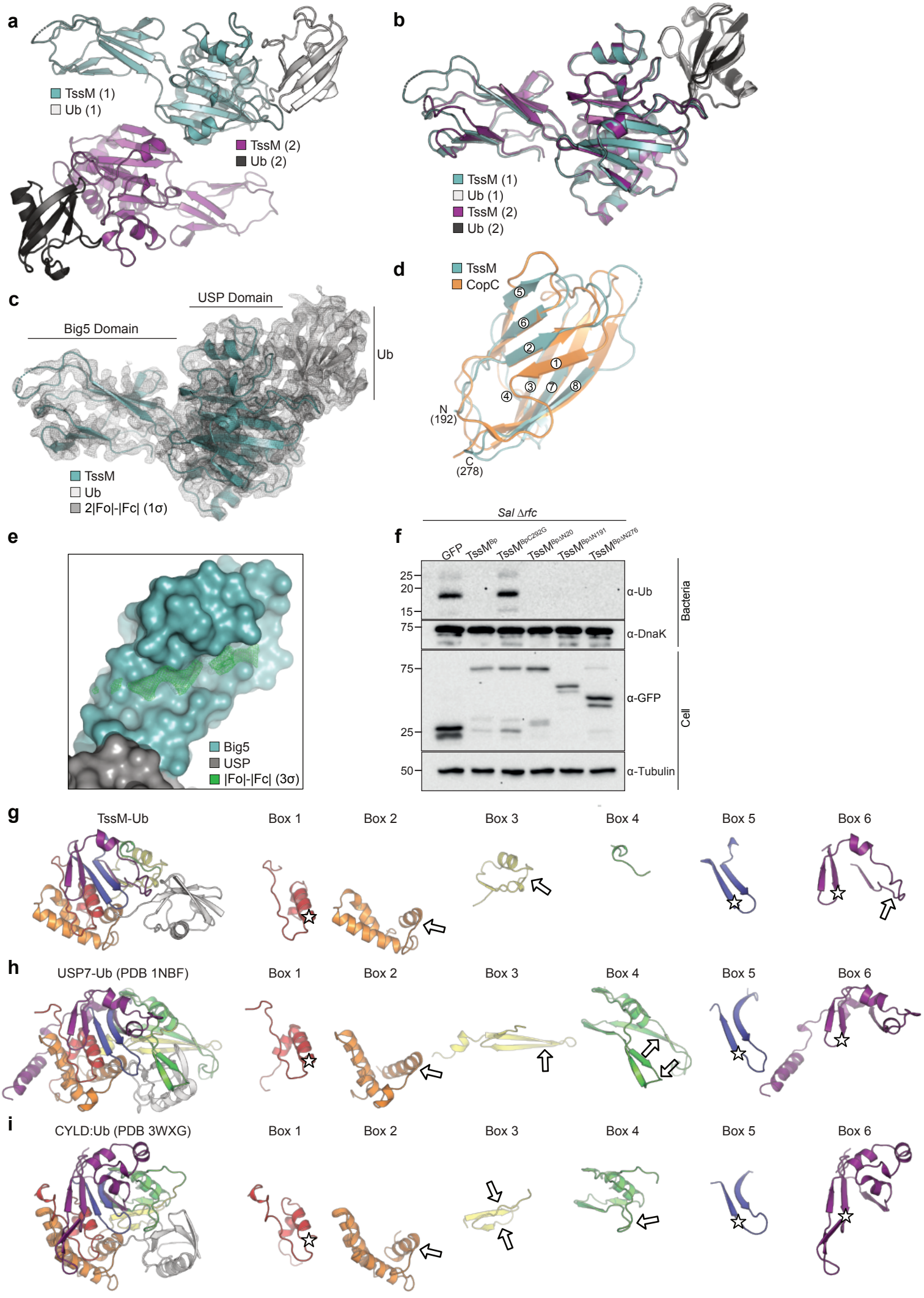

Extended Data Fig. 4: Structural basis of TssM esterase activity. a) Overview of the two TssM-Ub copies within the asymmetric unit of the determined crystal structure. **b)** Overlay of the two TssM-Ub complexes. Complex #1, which allowed for more complete modelling of the Big5 domain, was selected for subsequent analysis. **c)** Full 2|Fo|-|Fc| electron density for the TssM-Ub complex, shown at 1σ. **d)** Overlay of the TssM Big5 domain (teal) aligned with the Ig-like domain from the bacterial copper protein CopC (PDB 6NFQ), the most homologous structure identified by DALI analysis[60]. Of note is the missing b1 strand in TssM, which could be encoded outside of the crystallised construct boundaries. **e)** Despite lacking a b1 strand, both copies of the TssM Big5 domain within the asymmetric unit contain mysterious positive difference density shown in green (|Fo|-|Fc| map shown at 3σ) that cannot be explained by either protein or buffer constituents, raising the possibility of a ligand that co-purified from *E. coli*. **f)** Analysis of Δ*rfc Salmonella* isolated from infected cells expressing GFP-tagged $TssM^{Bp}$ WT or mutants, $TssM^{BpΔN20}$, $TssM^{BpΔN191}$ and $TssM^{BpΔN276}$. **g)** Structural breakdown of TssM Boxes 1-6, with catalytic triad residues indicated by stars and Ub-contacting regions indicated by arrows. **h)** As in g, for the human USP-type DUB USP7 (PDB 1NBF). **i)** As in g, for the human USP-type DUB CYLD (PDB 3WXG).

Extended data Fig 5.

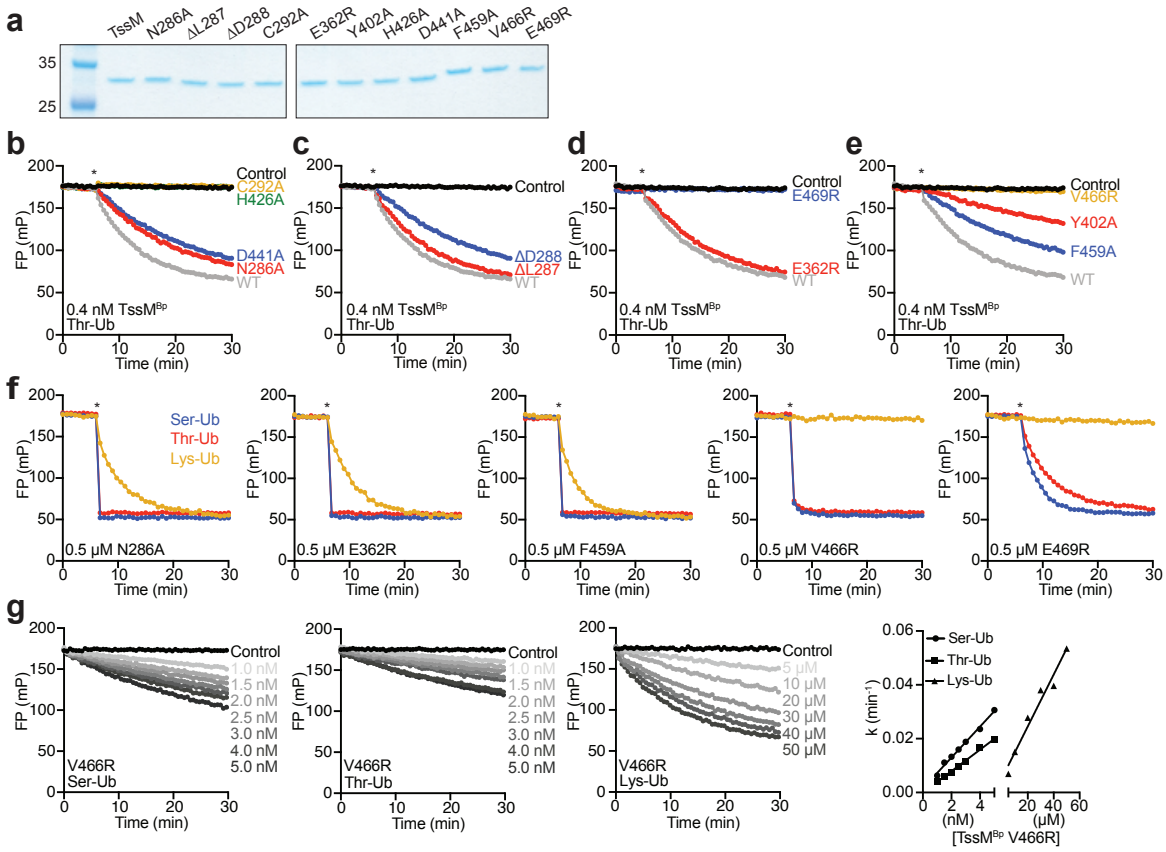

Extended Data Fig. 5: TssM^{Bp} mutants retain activity. a) Coomassie-stained gel showing purified TssM^{Bp} constructs used in FP experiments. **b-e)** TssM activity data for the Thr-Ub substrate with **b)** active site mutations, **c)** Cys-loop truncations, **d)** S1-site acidic mutations, and **e)** hydrophobic residue mutations. In all panels, 0.4 nM TssM^{Bp} was used to compare mutants to WT activity and graphs show a representative plot of data collected in triplicate. Addition of the DUB is indicated by an asterisk. WT and control data in b,c and d,e are identical and reproduced for clarity as data were collected in the same experiment. **f)** Representative FP data for the indicated TssM mutants at 0.5 μM for Ser-Ub (blue), Thr-Ub (red), and Lys-Ub (orange) substrates. The higher concentration for N286A, E362R, and F459A showed cleavage of all three substrates, while V466R and E469R retained esterase activity more than isopeptidase activity. The near immediate cleavage of the ester-linked Ser-Ub and Thr-Ub substrates prompted the selection of V466R over E469R as an esterase-specific mutant. Addition of the DUB is indicated by an asterisk. **g)** V466R nearly eliminates TssM^{Bp} isopeptidase activity. FP curves for the indicated concentrations of TssM^{Bp} V466R are shown for the cleavage of 50 nM Ub-Ser, Ub-Thr, and Ub-Lys substrates and are representative of three independent replicates.

Extended data Fig 6.

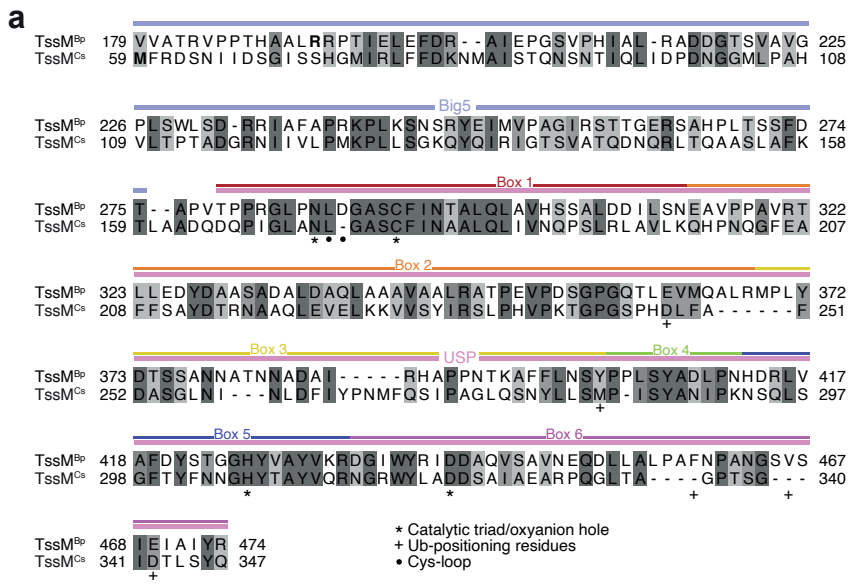

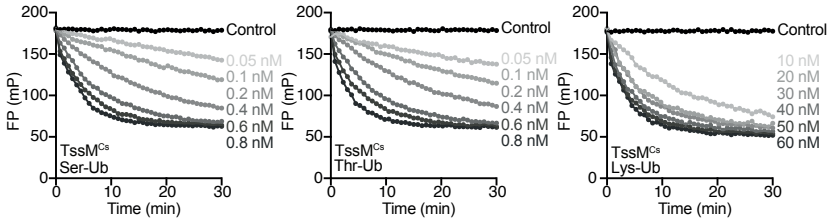

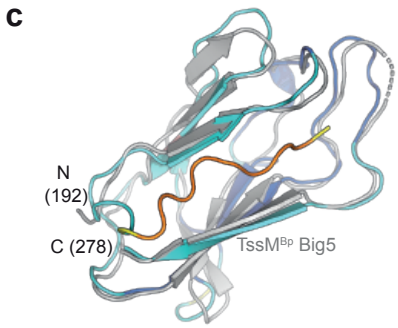

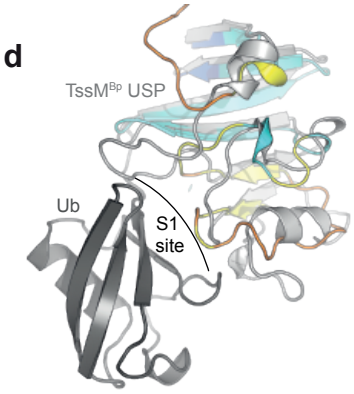

Extended Data Fig. 6: *Chromobacterium* TssM homologs retain esterase activity. a) Sequence alignment of the Big5 and USP domains from $TssM^{Bp}$ and a *Chromobacterium sinusclupearum* orthologue ($TssM^{Cs}$). Sequences were aligned using NCBI BLAST and visualised using Jalview[61]). Sequence identity and conservation parameters were each set to 50% and are shown in grey boxes, where the darkest grey denotes the highest degree of conservation and lighter shades denote decreasing conservation. The Big5 and USP domain boundaries are represented by pale purple and pale pink lines, respectively. For the USP domain, the boundaries of the six boxes are shown and are coloured accordingly. The N-termini for constructs used in our study for both $TssM^{Bp}$ and $TssM^{Cs}$ are marked in bold (R192 and M59, respectively). Point mutations for $TssM^{Bp}$ used in Fig. 3 and Extended Data Fig. 4 are denoted and labelled. Interestingly, most point mutations selected in $TssM^{Bp}$ are identical or highly conserved in $TssM^{Cs}$. Uniquely, $TssM^{Bp}$ features an insertion in the Cys-loop (D288), while $TssM^{Cs}$ encodes a shorter Cys-loop consistent with human USPs. Further, the S1 site of $TssM^{Bp}$ contains regions of inserted sequence when compared to $TssM^{Cs}$, where F459 and V466 have no homology in $TssM^{Cs}$. **b)** $TssM^{Cs}$ (59-347) was expressed and purified as described for $TssM^{Bp\Delta N191}$ and used in FP experiments to monitor esterase and isopeptidase activity. Data were collected over a range of indicated concentrations for Ser-Ub, Thr-Ub, and Lys-Ub substrates and were used to derive rate constants and catalytic efficiencies. **c)** Structural alignment of the Big5 domain for $TssM^{Bp}$ and $TssM^{Cs}$. $TssM^{Bp}$ is shown in light grey (residues 192-278) along with the AlphaFold model of $TssM^{Cs}$. Colouring of the $TssM^{Cs}$ model signifies standard AlphaFold confidence in the prediction such that a per-residue confidence score (pLDDT) > 90 is blue (very high), 90 > pLDDT > 70 is cyan (confident), 70 > pLDDT > 50 is orange (low), and pLDDT < 50 is yellow (very low). Overall the model aligns well to the TssM structure, with the exception of the most N-terminal ~10 residues which AlphaFold modelled with very low confidence. This region curiously resembles the extra electron density observed in our TssM data (Extended Data Fig. 3e). **d)** Structural alignment of the S1 site for $TssM^{Bp}$ and $TssM^{Cs}$. Low confidence modelling of the S1 site from $TssM^{Cs}$ highlights differences between it and $TssM^{Bp}$, namely a lack of defined secondary structure elements and the Box 6 blocking loop present in $TssM^{Bp}$.

Extended data Fig 7.

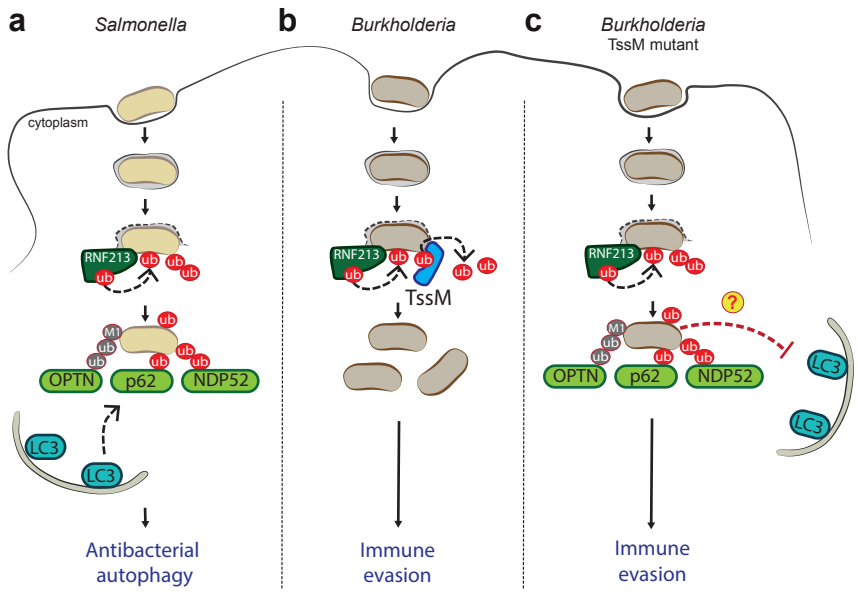

Extended Data Fig. 7: Schematic illustrating how *Burkholderia* evades RNF213-dependent restriction. **a**) Upon sporadic vacuole rupture, around 10% of *Salmonella* enter the host cell cytosol. These cytosolic bacteria are detected and ubiquitylated by RNF213, which triggers the recruitment of ubiquitin-binding autophagy receptors OPTN (Optineurin), p62, NDP52 and the autophagy marker LC3. This results in the growth restriction of cytosolic *Salmonella* by antibacterial autophagy. **b)** The cytosol-adapted pathogen, *Burkholderia,* which escapes into the host cytosol, is also detected by RNF213. However, *Burkholderia* effector TssM, an esterase and isopeptidase, directly counteracts RNF213 activity by hydrolysing ubiquitylated LPS. This prevents the recruitment of autophagy receptors and allows bacteria to replicate freely in the host cytosol. **c)** Without TssM, cytosolic bacteria become coated in ubiquitin and autophagy receptors in an RNF213-dependent manner. In contrast to *Salmonella*, *Burkholderia* blocks LC3 recruitment to evade antibacterial autophagy in a TssM-independent manner.